

yucca6, a Dominant Mutation in Arabidopsis, Affects Auxin Accumulation and Auxin-Related Phenotypes^{1[W][OA]}

Jeong Im Kim, Altanbadralt Sharkhuu, Jing Bo Jin, Pinghua Li, Jae Cheol Jeong, Dongwon Baek, Sang Yeol Lee, Joshua J. Blakeslee, Angus S. Murphy, Hans J. Bohnert, Paul M. Hasegawa, Dae-Jin Yun, and Ray A. Bressan*

Center for Plant Environmental Stress Physiology (J.I.K., A.S., J.B.J., P.M.H., R.A.B.) and Department of Horticulture and Landscape Architecture (J.J.B., A.S.M.), Purdue University, West Lafayette, Indiana 47906–2010; Department of Plant Biology, University of Illinois, Urbana, Illinois 61801 (P.L., H.J.B.); and Environmental Biotechnology National Core Research Center and Division of Applied Life Science (BK21 Program), Graduate School of Gyeongsang National University, Jinju 660–701, Korea (J.C.J., D.B., S.Y.L., D.-J.Y.)

Auxin plays critical roles in many aspects of plant growth and development. Although a number of auxin biosynthetic pathways have been identified, their overlapping nature has prevented a clear elucidation of auxin biosynthesis. Recently, *Arabidopsis* (*Arabidopsis thaliana*) mutants with supernormal auxin phenotypes have been reported. These mutants exhibit hyperactivation of genes belonging to the *YUCCA* family, encoding putative flavin monooxygenase enzymes that result in increased endogenous auxin levels. Here, we report the discovery of fertile dominant *Arabidopsis* *hypertall1-1D* and *hypertall1-2D* (*yucca6-1D*, *-2D*) mutants that exhibit typical auxin overproduction phenotypic alterations, such as epinastic cotyledons, increased apical dominance, and curled leaves. However, unlike other auxin overproduction mutants, *yucca6* plants do not display short or hairy root phenotypes and lack morphological changes under dark conditions. In addition, *yucca6-1D* and *yucca6-2D* have extremely tall (>1 m) inflorescences with extreme apical dominance and twisted cauline leaves. Microarray analyses revealed that expression of several indole-3-acetic acid-inducible genes, including *Aux/IAA*, *SMALL AUXIN-UP RNA*, and *GH3*, is severalfold higher in *yucca6* mutants than in the wild type. Tryptophan (Trp) analog feeding experiments and catalytic activity assays with recombinant *YUCCA6* indicate that *YUCCA6* is involved in a Trp-dependent auxin biosynthesis pathway. *YUCCA6:GREEN FLUORESCENT PROTEIN* fusion protein indicates *YUCCA6* protein exhibits a nonplastidial subcellular localization in an unidentified intracellular compartment. Taken together, our results identify *YUCCA6* as a functional member of the *YUCCA* family with unique roles in growth and development.

Auxins are crucial for plant viability and development. Numerous physiological studies indicate that the major naturally occurring auxin, indole-3-acetic

acid (IAA), functions in a plethora of important aspects of plant development and growth, including apical dominance, tropic responses to light and gravity, root and shoot architecture, vascular differentiation, embryo patterning, and shoot elongation (Davies, 2004). Changes in endogenous auxin levels induce genes such as *SMALL AUXIN-UP RNAs* (*SAURs*), *GH3*-related transcripts, and *Aux/IAA* family members via the TIR1/AFB receptor mechanism (Dharmasiri et al., 2005; Kepinski and Leyser, 2005). The movement of auxin through the plant, especially by polar transport mechanisms, has been the interest of classical and current studies aimed at understanding the function of this important hormone. The quantitative temporal and spatial distributions of IAA are crucial to accomplish appropriate growth and development (Muday and DeLong, 2001; Swarup and Bennett, 2003; Blakeslee et al., 2005). Although the IAA pools could be maintained at appropriate levels via auxin biosynthesis, conjugation, degradation, and transport mechanisms, de novo biosynthesis is the primal step to achieve the crucial level of auxin. However, our understanding of auxin biosynthesis is still particularly incomplete.

Analytical and feeding studies have described in exquisite detail where IAA and related compounds

¹ This work was supported by the National Science Foundation (grant nos. DBI-0223905 to H.J.B and MCB-0424850 to A.S.M.), by the Biogreen 21 project of the Rural Development Administration (grant no. 20070301034030), by the Basic Science Project of the Korea Science and Engineering Foundation (KOSEF; grant no. RO1-2006-000-10123-0), by the Environmental Biotechnology National Core Research Center Project of KOSEF (grant no. R15-2003-012-01002-00), by the Brain Korea 21 Program, Ministry of Education and Human Resources Development, Korea (scholarship to J.C.J.), and by Futuregene. Microscopy data was acquired in the Purdue Cancer Center Analytical Cytometry Laboratories supported by the Cancer Center NCI core grant no. NIH NCI-2P30CA23168. This work is Purdue University Agricultural Research Program Paper 2007-18193.

* Corresponding author; e-mail bressan@hort.purdue.edu.

The author responsible for distribution of materials integral to the findings presented in this article in accordance with the policy described in the Instructions for Authors (www.plantphysiol.org) is: Ray A. Bressan (bressan@hort.purdue.edu).

^[W] The online version of this article contains Web-only data.

^[OA] Open Access articles can be viewed online without a subscription.

www.plantphysiol.org/cgi/doi/10.1104/pp.107.104935

accumulate (Ljung et al., 2001, 2005), but application of these techniques to screens of loss-of-function mutants have not yielded enough information to fully characterize overlapping IAA biosynthetic pathways. Other efforts to dissect these pathways in *Arabidopsis thaliana* have focused on isolation of mutants that are resistant to exogenously applied auxins. This approach has been highly successful for the identification of auxin receptors and elucidation of auxin signaling pathways (Estelle and Somerville, 1987; Hellman et al., 2003; Yang et al., 2004), but has contributed less to elucidating IAA biosynthetic pathways.

A more productive avenue of research has been the identification and characterization of loss-of-function mutants exhibiting altered growth phenotypes. Auxin overproduction mutants such as *supperroot1* (*sur1*) and *sur2* have been identified and characterized from *Arabidopsis*. All these mutants were isolated from loss-of-function screening, because the loss of their functions attenuates depletion of auxin levels (Bak et al., 1998, 2001; Mikkelsen et al., 2000), indicating that gene products involved directly in auxin biosynthesis may be redundant.

Recently, application of a gain-of-function approach, activation tagging, in *Arabidopsis* has led to breakthroughs in the study of IAA biosynthesis. In independent efforts, activation tagging revealed five loci in *Arabidopsis* that encode proteins affecting auxin biosynthesis (Zhao et al., 2001; Marsch-Martinez et al., 2002; Woodward et al., 2005). These loci have been categorized into the *YUCCA* family of flavin monooxygenase (FMO)-like proteins. This family includes 11 members in the *Arabidopsis* genome (Zhao et al., 2001; Cheng et al., 2006). All the activation-tagged *yucca* mutants studied exhibit signature phenotypes found in auxin overproduction mutants such as *sur1* and *sur2*, and transgenic plants that overexpress the *Agrobacterium tumefaciens* phytohormone-biosynthetic gene *iaaM* (Zhao et al., 2001; Marsch-Martinez et al., 2002; Woodward et al., 2005). The proposed function of the *YUCCA* family of proteins in auxin biosynthesis has been further verified by Cheng et al. (2006). Double, triple, and quadruple mutants of *YUCCA* family members display dramatic developmental defects that are rescued by the bacterial auxin biosynthesis gene *iaaM*. This reverse genetic study along with previous work by Zhao et al. (2001) has revealed not only the functional redundancy but also some functional and physiological specificities among *YUCCA* members. Furthermore, the involvement of *YUCCA* in auxin biosynthesis has also been shown in rice (*Oryza sativa*) and petunia (*Petunia hybrida*; Tobeña-Santamaria et al., 2002; Yamamoto et al., 2007). Although it is clear that the *YUCCA* genes play critical roles in maintaining auxin levels in plants, their cellular and biochemical characteristics and specific functions of each family member have not been fully elucidated. The auxin biosynthetic pathway has been suggested to function in the cytoplasm although no demonstration of this

has been reported. In addition, although *YUCCA1* recombinant protein was reported to have enzymatic activity, no reports of catalytic functions of other *YUCCA* proteins have appeared.

Here, we report the dominant mutants *hypertall1-1D* (*hyt1-1D*)/*yucca6-1D* and *hyt1-2D*/*yucca6-2D* as new alleles of a member of the *YUCCA* family. Overexpression of the *YUCCA6* gene leads to elevated auxin levels and hyperinduction of several IAA-responsive genes. Although *yucca6-1D* displays some of the signature phenotypes common to other *Arabidopsis yucca* mutants, it also exhibits unique characteristics such as a normal root phenotype, an exceptionally large increase in inflorescence height, and altered leaf morphology. Recombinant *YUCCA6* protein appears to localize in a cytoplasmic compartment and can catalyze oxygenation of tryptamine, and, thus, *YUCCA6* appears to function in Trp-dependent auxin biosynthesis.

RESULTS

Isolation of the *hyt1-1D* Mutant

The *hyt1-1D* mutant was identified in a root-bending, second-site suppression mutation screen of a T-DNA insertion population (pSKI015) in the *Arabidopsis* Columbia (Col-0) *gl1 sos3-1* background (Rus et al., 2001; Miura et al., 2005). T3 individual lines of *sos3-1 hyt1-1D* were retested for salt sensitivity as described previously (Rus et al., 2001), and *sos3-1 hyt1-1D* exhibited slightly longer roots with or without salt added to the medium. Therefore, *sos3-1 hyt1-1D* was not included in further characterizations of *sos3-1* suppression lines. However, during production of T3 lines, it was evident that *sos3-1 hyt1-1D* plants displayed dramatic developmental alterations compared to the wild type. Eight weeks after germination, plants of *sos3-1 hyt1-1D* had only one inflorescence, whereas wild-type plants of the same age had at least five (Fig. 1A). Although *sos3-1 hyt1-1D* mutants eventually formed floral branches, the height of fully grown *sos3-1 hyt1-1D* plants was over twice that of wild-type plants. From an F₂ population of the backcross of *sos3-1 hyt1-1D* to Col-0 *gl1*, a single mutant, *hyt1-1D*, was isolated. The *hyt1-1D* mutant displayed the same morphological and developmental phenotypes as *sos3-1 hyt1-1D* (Figs. 1A and 2). Therefore, *hyt1-1D* was used for further investigations. The F₂ generation progeny of the *hyt1-1D* and Col-0 *gl1* crossed line showed a segregation of the *hyt1-1D*:wild-type phenotypes of 3:1 ($\chi^2 = 0.043$; $P > 0.05$), indicating that the *hyt1-1D* mutation was in a dominant single nuclear locus (Table I).

Identification of the T-DNA Insertion Position in the *hyt1-1D* Mutant

The genomic DNA adjacent to the left border of the T-DNA insertion was cloned by thermal asymmetric

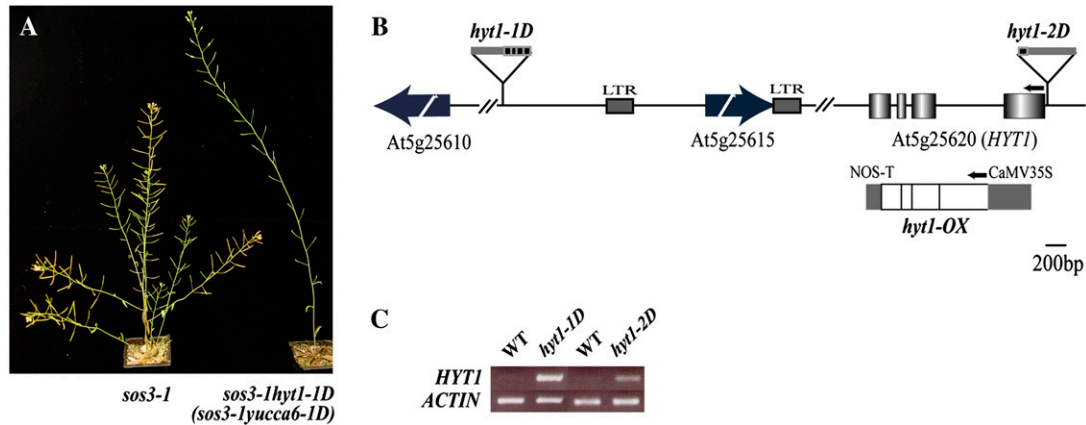


Figure 1. Identification of the T-DNA insertion sites and transcript level changes in *sos3-1 hyt1-1D* (*sos3-1 yucca6-1D*) and *sos3-1 hyt1-2D* (*sos3-1 yucca6-2D*). **A**, Morphological phenotypes of *sos3-1 hyt1-1D*. *sos3-1*, wild-type plant (left), and *sos3-1 hyt1-1D* (*sos3-1 yucca6-1D*; right) grown on soil for 8 weeks are shown. **B**, Gene organization of *HYT1* (*YUCCA6*) and schematic representation of T-DNA insertion alleles are illustrated. Arrow boxes indicate predicted genes near T-DNA insertion position. Boxes represent exons, and the intervening lines denote introns. The location of T-DNA insertion in alleles of *hyt1-1D* (*yucca6-1D*) and *hyt1-2D* (*yucca6-2D*) are shown as boxes above the genomic structures. The arrows above the genomic structure denote the direction of translation. Overexpression construct for ORF is shown below the genomic region of *HYT1*. NOS, Nopaline synthase. **C**, *HYT1* (*YUCCA6*) expression levels in *hyt1-1D* (*yucca6-1D*) and *hyt1-2D* (*yucca6-2D*) compared with the wild type were shown in RT-PCR analysis. Total RNA was extracted from 4-week-old mature rosette leaves of wild type and mutants. *ACTIN* was used as a control for loading.

interlaced-PCR. Perfectly matched sequences were found in the bacterial artificial chromosome clone T14C9. The left border of the T-DNA was inserted at 84,710 nucleotides from the 5' end of T14C9. The open reading frame (ORF) near the left border of the T-DNA encodes a product (*At5g25610*) with high similarity to RD22 (Fig. 1B). The distance between the T-DNA insertion and the translation start site of this ORF is about 10 kb. No transcriptional change in *At5g25610* between the wild type and the *hyt1-1D* mutant was detected by reverse transcription (RT)-PCR (data not shown), suggesting that *At5g25610* is not involved in the *hyt1-1D* phenotype. The ORF of the right border of the T-DNA insertion encodes a copia-like retrotransposon (*At5g25615*; Fig. 1B). The distance between the cauliflower mosaic virus (CaMV) 35S enhancers and the predicted translation start site is about 1.2 kb. Both the 5' and 3' ends of *At5g25615* have 337 bp of long terminal repeat (LTR) sequences. Transcripts of *At5g25615* as well as the LTR regions accumulated slightly more in *hyt1-1D* compared to the wild type (data not shown). However, introducing into the wild-type plants either cDNA of *At5g25615*, the LTR region, or the genomic region including the LTR under the control of the CaMV 35S promoter could not recapitulate any phenotype of *hyt1-1D* (data not shown), indicating that altered expression of neither *At5g25615* nor the LTR regions could cause *hyt1-1D* phenotypes.

Identification of the *HYT1* Locus

From the result of microarray analyses, we found that the accumulation of transcript of an FMO

(*At5g25620*; GenBank accession no. NC_003076) in the mutant was 9.8-fold higher than in the wild-type plant (Table II). The distance between the CaMV 35S enhancers and the predicted translation start site of *At5g25620* was about 11 kb. RT-PCR confirmed that the transcript of this FMO-like gene accumulated to high levels in *hyt1-1D* (Fig. 1C), indicating that overexpression of the FMO-like protein could be the locus responsible for the *hyt1-1D* phenotypes.

From the Salk Institute Genome Analysis Laboratory database (Alonso et al., 2003), we identified SALK_019589 that was revealed by diagnostic PCR to have a T-DNA insertion that included an intact 35S promoter in the 5'-untranslated region of *At5g25620*. Transcript of the FMO in SALK_019589 also accumulated to a high level compared to that in wild-type plants (Fig. 1C). SALK_019589 also displayed similar morphological phenotypes as *hyt1-1D* (Fig. 2A). *At5g25620* was annotated as *HYT1*, and SALK_019589 was designated as *hyt1-2D* as an allele of *HYT1*.

HYT1 Is a Member of the *YUCCA* Gene Family

Sequence analysis of the *HYT1* cDNA clone showed that it encodes a 418-amino acid putative flavin-containing monooxygenase. Phylogenetic tree analysis indicated that *HYT1* is one of 11 Arabidopsis *YUCCA*-like family genes and belongs to the *YUCCA2* subfamily (Cheng et al., 2006). In comparison with other *YUCCA* family genes, *HYT1* has 48.5% amino acid identity with *YUCCA1* and 61.0% amino acid identity with *YUCCA2* (data not shown). The ORFs of *HYT1*, *YUCCA1*, and *YUCCA2* from Arabidopsis and

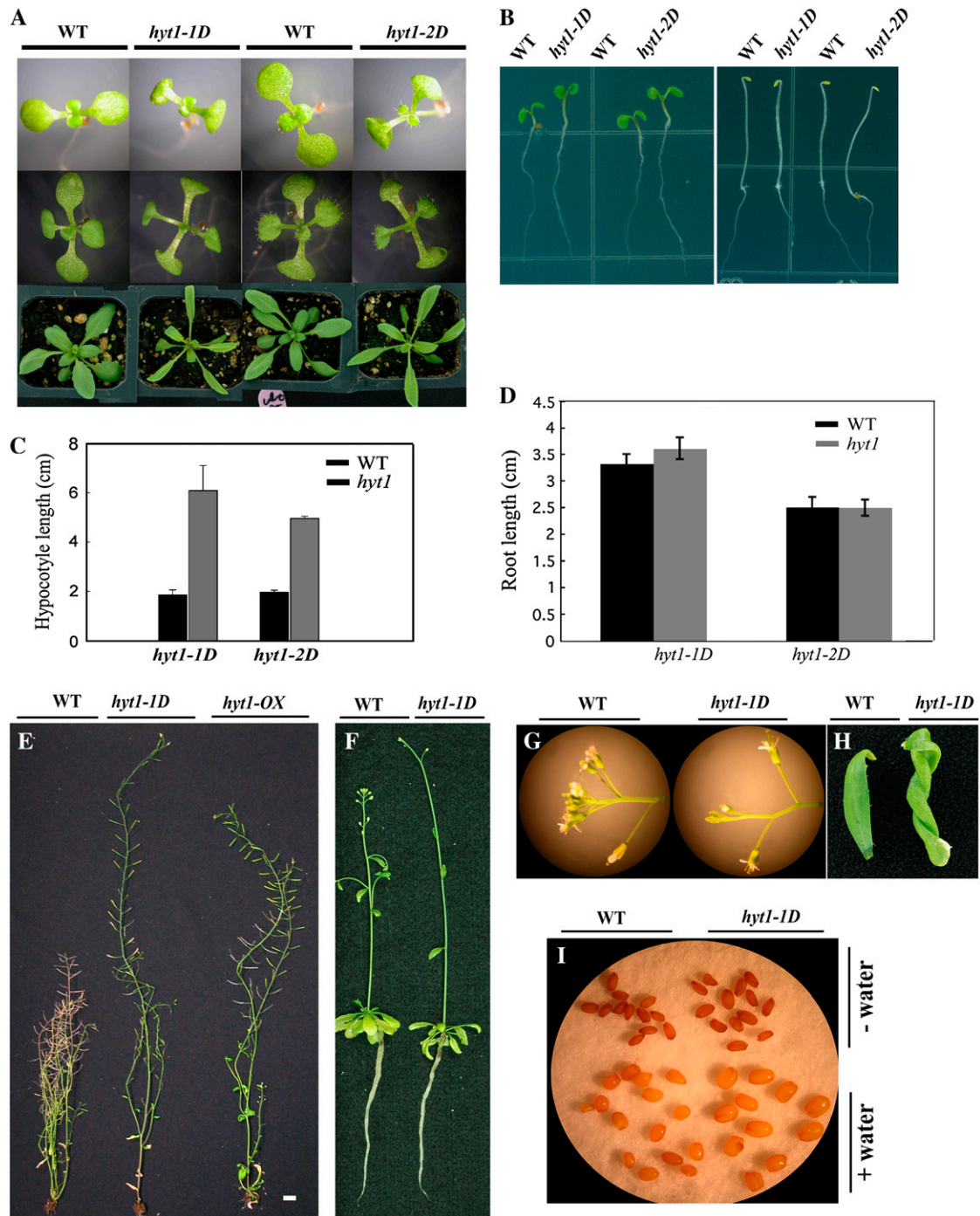


Figure 2. Analysis of the *hyt1-1D* (*yucca6-1D*) and *hyt1-2D* (*yucca6-2D*) phenotypes. A, *hyt1-1D* (*yucca6-1D*) and *hyt1-2D* (*yucca6-2D*) plants with their wild-type plants, Col-0 *gl1* and Col-0, respectively, grown for 7 d and 14 d on MS medium or 25 d on soil (from top row to bottom row). B, *hyt1-1D* (*yucca6-1D*) and *hyt1-2D* (*yucca6-2D*) plants grown on MS media for 4 d in light (left) and dark (right) conditions compared with their wild types. C, Hypocotyl length of *hyt1-1D* (*yucca6-1D*) and *hyt1-2D* (*yucca6-2D*) seedlings grown for 10 d on MS media containing 0.8% (w/v) agar compared with their wild types. Black bar is the wild type and gray bar is the mutant, $n = 20$. D, Root length of *hyt1-1D* (*yucca6-1D*) and *hyt1-2D* (*yucca6-2D*) seedlings grown for 7 d (*yucca6-1D*) and 6 d (*yucca6-2D*) on MS media containing 1.2% (w/v) agar compared with their wild types. Black bar is the wild type and gray bar is the mutant, $n = 15$. E, Six-week-old mature plants of wild type, *hyt1-1D*, and *hyt1-OX*, a transgenic plant with overexpressed transcripts of *HYT1* (from left to right, respectively). Scale bar = 2 cm. F, Roots of wild-type and *hyt1-1D* (*yucca6-1D*) plants grown in hydroponic culture condition. Soil-grown 2.5-week-old seedlings were transferred to the hydroponic solution and photographed 21 d after growth in hydroponic solution. G, Flowers of wild-type (left) and the *hyt1-1D* (*yucca6-1D*) plants (right). H, Cauline leaf of 2-month-old wild-type (left) and *hyt1-1D* (*yucca6-1D*) plants (right). I, Seeds of wild type (left) and *hyt1-1D* (*yucca6-1D*); right) before (top) and after imbibing water (bottom) for 4 d.

FLOOZY (*FLZ*) from petunia are intercepted by three introns. Similar to *YUCCA1*, *YUCCA5*, and *FLZ*, the *HYT1* protein contains conserved binding motifs (GAGPSG) for FAD and (GCGNSG) for NADPH (data not shown). *HYT1* and *hyt1-1D*, *hyt1-2D* were renamed *YUCCA6* and *yucca6-1D*, *yucca6-2D*, respectively, following the nomenclature of the *YUCCA* family genes.

Overexpression of *YUCCA6* Recapitulates the *yucca6-1D* Phenotype

To confirm whether overexpression of *YUCCA6* caused the *yucca6* mutant phenotypes, the cDNA of *YUCCA6* was introduced under the control of the constitutive CaMV 35S promoter into wild-type plants, causing overexpression of *YUCCA6* transcript (Figs. 1B and 3C). As shown in Figures 2E and 3, A and B, transgenic plants exhibited *yucca6* mutant phenotypes such as epinastic cotyledons, long hypocotyls, long narrow leaves with elongated petioles, and strong apical dominance. These results confirmed that phenotypes observed in *yucca6-1D* and *yucca6-2D* result from the enhanced accumulation of *YUCCA6* transcript.

The Dominant Mutation of *YUCCA6* Confers Traits Unique among *YUCCA* Family Members

Homozygous *yucca6-1D* and *yucca6-2D* plants showed pleiotropic effects at several stages of plant development. Both *yucca6-1D* and *yucca6-2D* seedlings exhibited epinastic cotyledons and narrow, long rosette leaves with downward curled edges, and elongated petioles (Fig. 2A). The hypocotyl lengths of *yucca6-1D* and *yucca6-2D* were 3.2 (*yucca6-1D*) and 2.5 times (*yucca6-2D*) longer than the wild-type seedlings, respectively, under long-day conditions (Fig. 2C). Mature plants produced a strong apically dominant inflorescence (Fig. 2E). Such phenotypes are very similar to IAA overproduction mutants, such as *yucca1*, *yucca4*, *FZYox*, *sur1*, *sur2*, and *CYP79B2ox* (Boerjan et al., 1995; King et al., 1995; Barlier et al., 2000; Zhao et al., 2001, 2002; Marsch-Martinez et al., 2002; Tobeña-Santamaria et al., 2002). However, several unique traits were observed in *yucca6* mutants. Although short, hookless, etiolated hypocotyls and short, hairy roots are other phenotypes commonly found in IAA overproduction mutants (Boerjan et al., 1995; Delarue et al., 1998; Zhao et al., 2001; Smolen and Bender, 2002; Tobeña-Santamaria et al., 2002), these phenotypes were not evident in *yucca6-1D* and *yucca6-2D* (Fig. 2B). Root length and lateral root number of *yucca6* seedlings were not different from the wild type when grown in solid Murashige and Skoog (MS) media or in hydroponic conditions (Fig. 2, B, D, and F). However, *yucca6* plants were at least twice as tall as wild-type plants (Fig. 2E). The pedicel length and distance between siliques on the main inflorescence of *yucca6-1D* mutants were longer than the wild type, and *yucca6-1D* had more bud clusters than the wild type (Fig. 2G).

The seed size of *yucca6-1D* was also slightly larger than the wild type, especially after imbibing water (Fig. 2I). In addition, mature cauline leaves of 8-week-old *yucca6-1D* were severely twisted (Fig. 2H).

Overexpression of *YUCCA6* Induces IAA-Regulated Genes and Elevates Auxin Levels

From microarray analyses, expression of several IAA-inducible genes, including *Aux/IAA*, *SAUR*, and *GH3*, was found to be severalfold higher in *yucca6* mutants than that in the wild type (Table II). The elevated transcript levels of *GH3* and *IAA1* were confirmed by RT-PCR analysis (Supplemental Fig. S1). Using the *DR5:GUS* maximal auxin reporter (Ulmasov et al., 1997), IAA levels were estimated by GUS staining in planta. Strong GUS expression in the cotyledon, rosettes, and hypocotyls in *DR5:GUS/yucca6-1D* was observed (Fig. 4, C–H), indicating increased endogenous IAA levels. In addition, the ability of elevated auxin levels in *yucca6-1D* to function physiologically in vivo was tested with an auxin dependency assay in callus culture. As shown in Figure 4B, when *yucca6-1D* explants were grown in MS medium, root growth was observed in *yucca6-1D* explants but not in wild-type explants. Also, *yucca6-1D* explants cultured in MS media containing cytokinin could produce callus and regenerate shoots, whereas wild-type explants could not (Fig. 4A). Endogenous free IAA levels were also measured in the *yucca6* mutant and in wild-type plants at different developmental stages and tissues. Five-day-old *yucca6* mutant seedlings contained similar amounts of free IAA compared to wild-type seedlings. Six-week-old upper inflorescences and cauline leaves of *yucca6* mutants also contained higher levels of auxin than wild-type plants (Fig. 5). However, free auxin levels in 10-d-old *yucca6* seedling roots were not different from the wild type. Free auxin was increased 25% in shoots. Inflorescences (including flowers) of *yucca6* mutants contained 32% more free IAA than the wild type, and the free IAA levels were increased 91% in cauline leaves, which had a dramatically altered morphological phenotype compared to the wild type (Figs. 5 and 2H). Thus, the organs exhibiting strong phenotypic alterations, such as cauline leaves and inflorescences, also exhibited the greatest increases in auxin levels, whereas the root system that did not exhibit any phenotype changes (Fig. 2, B, D, and F) showed no significant changes in auxin levels.

YUCCA6 Is Involved in a Trp-Dependent IAA Biosynthesis Pathway

It has been proposed that plants use Trp-dependent and Trp-independent routes to synthesize auxin (Normanly et al., 1993; Müller and Weiler, 2000; Woodward and Bartel, 2005). To investigate in which pathway *YUCCA6* may participate, we tested the resistance of *yucca6-1D* and *yucca6-2D* to the toxic Trp

Table I. Genetic analysis of *hyt1-1D* (*yucca6-1D*) F_2 progeny of *hyt1-1D* (*yucca6-1D*) \times wild-type line

Phenotype was determined by leaf morphology and apical dominance; +, having mutant phenotypes; -, having wild-type phenotypes. The χ^2 value is for an expected ratio of 3:1 (*hyt1-1D* [*yucca6-1D*]:wild type). $\chi^2_{0.05} = 3.841$.

Cross	Progeny	Total	Phenotype		χ^2
			1	2	
<i>hyt1-1D</i> (<i>yucca6-1D</i>) \times wild type	F ₁	64	64	0	0.043 (<3.841)
	F ₂	401	299	102	

analog, 5-methyl-Trp. When *yucca6-1D* and *yucca6-2D* were grown in MS medium containing 80 μ M 5-methyl-Trp, *yucca6-1D* and *yucca6-2D* could survive and grow, whereas wild-type plants could not (Fig. 6, A and B), indicating that *YUCCA6* is involved in Trp-dependent auxin biosynthesis.

It has been reported that maltose-binding protein (MBP):*YUCCA1* fusion proteins have catalytic activity to convert tryptamine to *N*-hydroxyl tryptamine (Zhao et al., 2001). To investigate if *YUCCA6* also is involved in oxidation of tryptamine, we tested *YUCCA6* activity with MBP:*YUCCA6* fusion protein expressed in and purified from bacteria. It is known that FMOs oxidize NADPH by transfer of electrons to oxygen. As shown in Figure 7, expressed *YUCCA6* has a K_m of approximately 0.274 mM and a V_{max} of 9.46 μ mol NADPH $\text{min}^{-1} \text{mg}^{-1}$ using tryptamine as a substrate. The catalytic activity of *YUCCA6* for oxidation of tryptamine, together with resistance of *yucca6* mutants to 5-methyl-Trp, strongly implies that *YUCCA6* has an important function in Trp-dependent auxin biosynthesis.

YUCCA6 Is Normally Expressed in Roots, Cauline Leaves, and Flowers

The transcript levels of *YUCCA6* in different organs of wild-type and *yucca6* mutant plants were investigated by RT-PCR. In the *yucca6-1D* plants, the transcript of *YUCCA6* was highly expressed in all the tissues tested, including roots and etiolated hypocotyls, where

no change in phenotypes was observed (Fig. 8). In wild-type plants, the transcript of *YUCCA6* was highly expressed in roots but modestly expressed in the cauline leaves and flowers, including bud clusters (Fig. 8). This is consistent with the expression profiles of *YUCCA6* (*At5g25620*) provided by AtGenExpress Visualization Tool (<http://jsp.weigelworld.org/expviz/expviz.jsp>; Schmid et al., 2005). The *YUCCA6* transcript levels indicate that the *YUCCA6* gene may be involved normally in auxin-mediated processes, mainly in roots. Overexpression of *YUCCA6* in *yucca6-1D* resulted in increased transcript levels of *YUCCA6* in several tissues but not in roots, where *YUCCA6* transcript is already very high in the wild type. As mentioned earlier, this may explain the lack of effect of activation of *YUCCA6* on root phenotypes. SALK_093708 was identified from the Salk Institute Genome Analysis Laboratory database, and the presence of a T-DNA insertion in the first intron of *At5g25620* was confirmed by diagnostic PCR analysis according to the SALK T-DNA verification protocol (<http://signal.salk.edu>). Transcript of *YUCCA6* was not detected in homozygous SALK_093708 plants under our conditions, suggesting that SALK_093708 is a loss-of-function mutation of *YUCCA6* (Supplemental Fig. S2D). We named SALK_093708 *yucca6-3k*. Homozygous *yucca6-3k* plants exhibited visible phenotypes opposite to *YUCCA6* overexpression mutants, such as wider rosette leaves (Supplemental Fig. S2, A and B) and decreased plant height at maturity compared to wild-type plants (Supplemental Fig. S2C). However, root morphology of

Table II. IAA response genes up-regulated in *sos3-1 hyt1-1D* (*sos3-1 yucca6-1D*) mutants

Fold mRNA accumulation in *sos3-1 hyt1-1D* (*sos3-1 yucca6-1D*) mutant versus the wild type (*sos3-1*) was determined by microarray hybridization.

AGI ID	Gene Title	Fold
At5g25620	FMO-like protein	9.8
At2g23170	Auxin-responsive GH3 family GH3.3	6.2
At5g54510	Auxin-responsive GH3 family GH3.6	4.4
At4g14560	IAA1	5.2
At4g32280	Aux/IAA family	3.8
At3g23050	IAA7	3.6
At4g38850	SAUR-AC1	3.1
At3g15540	IAA19	3.1
At3g23030	IAA2	3.0
At5g18030	Auxin-inducible SAUR	3.0
At5g18050	Auxin-inducible SAUR	2.9
At5g18020	Auxin-inducible SAUR	2.9
At5g18010	Auxin-inducible SAUR	2.7

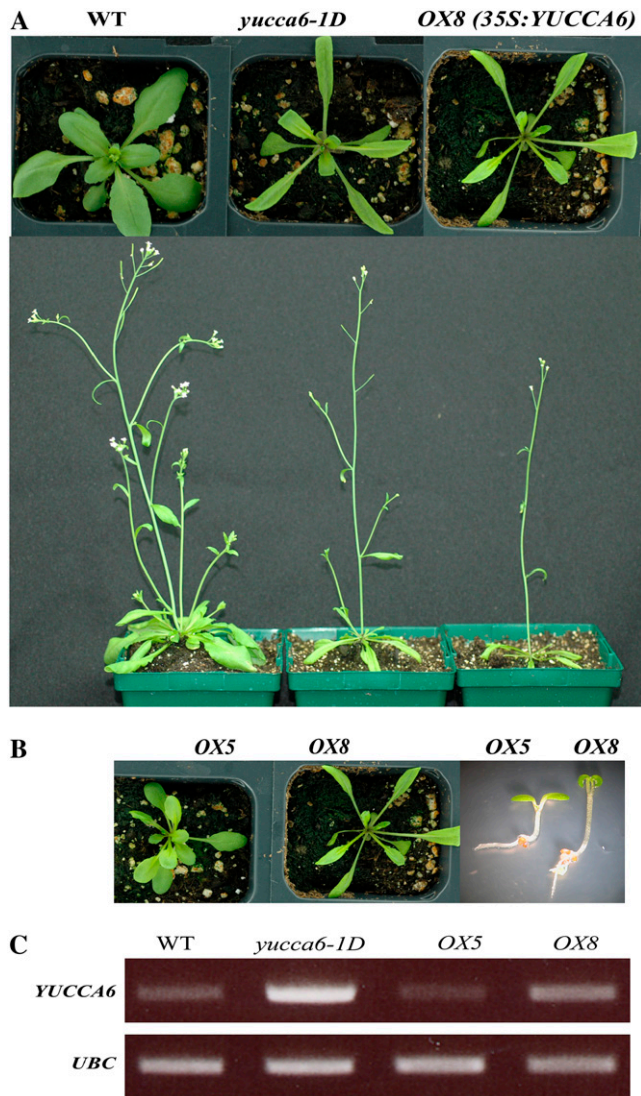


Figure 3. Expression of *YUCCA6* cDNA driven by the CaMV 35S promoter recapitulated the *yucca6-1D* phenotype. A, Mature plants of 3-week-old (top) and 4-week-old (bottom) wild-type, *yucca6-1D*, and transgenic plants expressing CaMV35S:*YUCCA6* (from left to right). B, Phenotypes of transgenic plants depend on expression level of *YUCCA6*. Both *OX5* and *OX8* are transgenic plants expressing CaMV35S:*YUCCA6*. Phenotypes of 3-week-old mature plants (left and middle) and 5-d-old seedlings (right) of *OX5* and *OX8* are shown. C, The expression levels of *YUCCA6* transcripts in wild type, *yucca6-1D*, *OX5*, and *OX8* were shown in RT-PCR analysis. *UBC* was used as a control for loading. PCR was performed for 35 cycles with 0.1 μ L of cDNA.

yucca6-3k was not distinctively different from wild-type roots (Supplemental Fig. S2E).

YUCCA6 Protein Is Localized in a Cytoplasmic Compartment

To elucidate subcellular localization of *YUCCA6* proteins, we constructed plasmids encoding *YUCCA6*:

GFP and *YUCCA6*:RFP (red fluorescent protein) fusion proteins driven by the 35S promoter, as described in "Materials and Methods." *YUCCA6*:GFP was transiently expressed in *Arabidopsis* protoplasts, and green fluorescent signals were observed by confocal microscopy. To confirm if *YUCCA6*:GFP fusion protein is functional or not, we analyzed the expression levels of the auxin-responsive *GH3* gene (*At2g23170*). Expression of *YUCCA6*:GFP promoted expression of *GH3*, but expression of GFP alone did not increase the

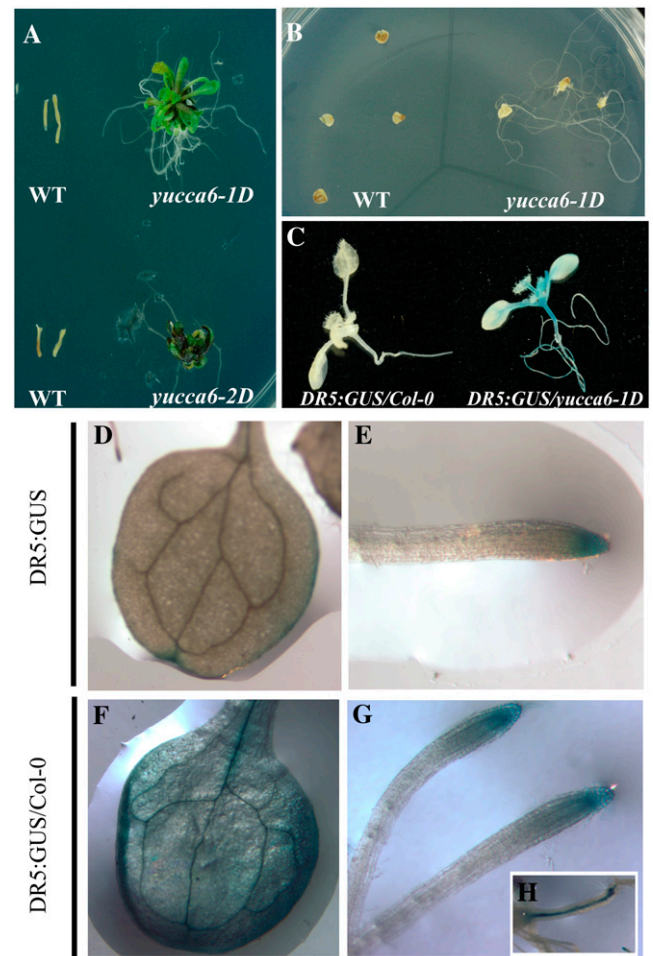


Figure 4. Endogenous auxin responses are elevated in *yucca6* mutants. Hypocotyl explants of *yucca6-1D* and *yucca6-2D* compared to their wild types grown on MS media containing 100 μ M kinetin for 3 weeks. Hypocotyl explants were taken from 2-week-old seedlings and cultured in 100 μ M kinetin-containing MS media for 3 weeks under a 16-h-light/8-h-dark cycle in the growth room. B, Cotyledon explants of *yucca6-1D* and the wild type on MS media for 3 weeks. Cotyledon explants were cultured in the same condition as hypocotyls explants. C, Induction of GUS activity in 2-week-old *DR5:GUS/Col-0* (left) and *DR5:GUS/yucca6-1D* (right). *DR5:GUS/Col-0* represents *Col-0* plants containing GUS reporter gene and *DR5:GUS/yucca6-1D* represents F₁ generation plant from *DR5:GUS* crossed with *yucca6-1D*. D and E, Cotyledon and root of *DR5:GUS/col-0*. F to H, Cotyledon, root, and hypocotyls of *DR5:GUS/yucca6-1D*.

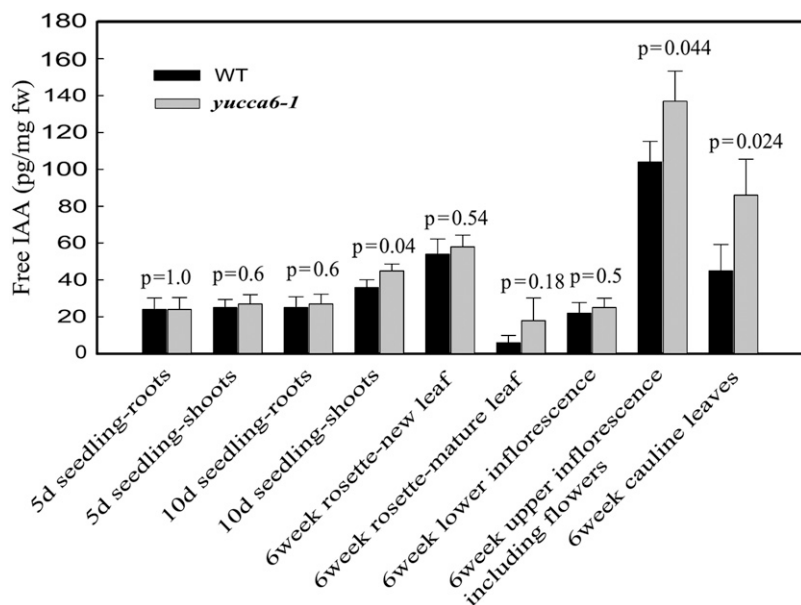


Figure 5. Free IAA measurement in different developmental stages and organs in *yucca6* mutant and wild type. Specified organ tissues from wild type and *sos3-1 yucca6-1D* mutant were harvested and used for free IAA measurement. Black bars represent wild type and gray bars represent mutant. Values are means and sds of three replicates. The *P* values are from a Student Newman Keuls post hoc ANOVA with $\alpha = 0.05$.

transcript level of *GH3* (Supplemental Fig. S3B). This result indicates that YUCCA6:GFP is functional.

Both YUCCA6:GFP and YUCCA6:RFP exhibited largely colocalized patterns of discrete spots of fluorescence. To identify the subcellular compartments where localization of YUCCA6 occurs, YUCCA6:GFP and YUCCA6:RFP were coexpressed with several organelle markers. F1-ATPase- γ :RFP was used to identify mitochondria (Jin et al., 2003), rat sialyltransferase:GFP was used to identify the Golgi apparatus (Jin et al., 2001), BiP:RFP was used to identify endoplasmic reticulum compartments (Jin et al., 2001), RFP:SKL was used to identify the peroxisome (Lee, et al., 2002), and chlorophyll autofluorescence was used to mark chloroplasts. As shown in Supplemental Figure S3A, YUCCA6:GFP/RFP fusions did not colocalize with any of these subcellular markers. YUCCA6 appears to function in the cytosol or in an unidentified endomembrane compartment.

DISCUSSION

YUCCA6 and Trp-Dependent Auxin Biosynthesis Pathway

IAA biosynthetic pathways have been extensively studied, but their complexity has not been elucidated in detail (Bartel et al., 2001; Woodward and Bartel, 2005). Understanding the genetic basis of auxin biosynthesis was significantly aided by the discovery of the gene activation mutants such as *yucca1*, *yucca4*, and *yucca5*. Although the function of Arabidopsis, rice, and petunia YUCCA homologous genes in auxin biosynthesis appear to be clear, the roles of each protein remain unknown. Zhao et al. (2001) provided evidence that recombinant YUCCA1 protein could catalyze the

conversion of tryptamine to *N*-hydroxyl tryptamine, suggesting the function of the YUCCA family in a Trp-dependent auxin biosynthesis pathway.

Our results have clearly demonstrated that YUCCA6 is also involved in the same step of a Trp-dependent auxin biosynthesis pathway. Overexpression of YUCCA6 causes typical auxin overproduction phenotypes and elevates the free IAA level enough to induce expression of auxin-responsive genes (Figs. 1–5). *yucca6-1D* and *yucca6-2D* mutants are resistant to the toxic Trp analog 5-methyl-Trp (Fig. 6). Recombinant YUCCA6 protein can catalyze the conversion of tryptamine to *N*-hydroxyltryptamine (Zhao et al., 2001; Fig. 7). Considering that tryptamine has not been detected in Arabidopsis (Woodward and Bartel, 2005), it is difficult to predict a reasonable physiological K_m for tryptamine oxidation. It may be that tryptamine is highly unstable in vivo or that another metabolite in this complex pathway is the natural substrate for YUCCA6. However, the apparent K_m that we measured for tryptamine is reasonable for normal cellular concentrations of amino acids and many of their metabolites (Bak and Feyereisen, 2001; Park et al., 2003). Also, the relative rates of oxidation using tryptamine or indoleacetonitrile (IAN) as substrate indicate a significantly greater affinity of YUCCA6 enzyme for tryptamine. This is consistent with the specific preference of human or yeast FMO enzymes for NH_2 or SH_2 groups over a $\text{N}\equiv\text{C}$ group, as is present on IAN. The precise specificity of YUCCA6 for various potential natural substrates and the biochemical characterization of other YUCCA proteins await more thorough investigation.

The Overlapping and Unique Function of YUCCA6

The fact that neither any of the *yucca* single mutants (*yucca1*, 2, 3, or 4) nor the *yucca1yucca2* double mutant

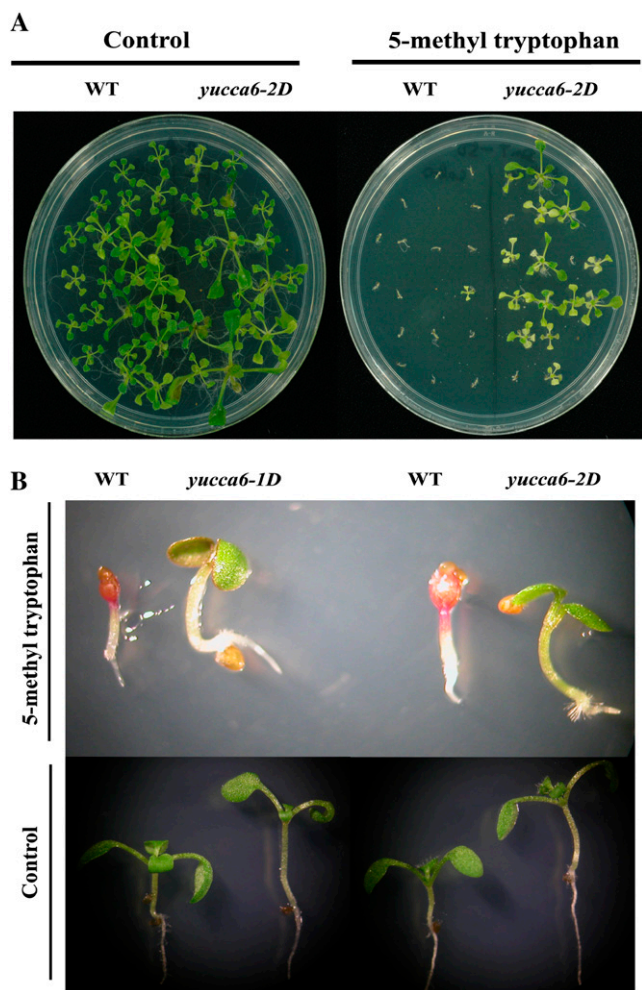


Figure 6. Response to a toxic analog of Trp, 5-methyl-Trp. A, Wild type and *yucca6-2D* grown on MS media without (left) and with 80 μM of 5-methyl-DL-Trp (right) for 3 weeks. B, Wild type and *yucca6* mutants grown on MS media without (bottom) and with 80 μM of 5-methyl-DL-Trp (top) for 8 d.

has obvious phenotypes (Zhao et al., 2001; Cheng et al., 2006) revealed the overlapping functions of members of the YUCCA family. Recently, several single, double, and even triple mutants of YUCCA family loci have revealed that at least double loci mutations are needed to manifest strong phenotypes (Cheng et al., 2006). We also observed only weak morphological phenotypes of the knockout mutant *yucca6-3k* (Supplemental Fig. S2A). This genetic redundancy among YUCCA family members could be the reason why no auxin-deficient mutants were found initially in screens for loss of auxin-mediated phenotypes.

The primary effect of auxin at the cellular level is to stimulate cell enlargement, yet no other plant hormone mediates more diverse aspects of whole plant phenotype than does auxin. Although auxin receptors have recently been identified and characterized (Dharmasiri et al., 2005; Kepinski and Leyser, 2005), many aspects of auxin signal transduction remain uncharacterized.

The regulation of auxin biosynthesis is also poorly described. Our results and previous reports lead us to consider that there are unique functions of YUCCA6 that may control diverse aspects of plant growth and development through de novo auxin biosynthesis. Arabidopsis YUCCA overexpression mutants that have been reported to date exhibit similar but not identical phenotypes. Recently, Cheng et al. (2006) made several double knockout mutants with various combinations of YUCCA1, 2, 4, and 6. They found that double mutations of genes belonging to the same clade cause severe development defects, whereas no dramatic phenotypes were observed with knockout combinations of genes from different clades, suggesting that genes that belong to the same clade may share greater overlapping functions (Cheng et al., 2006). The phenotype of *yucca6* mutants further advances the hypothesis that the existence of the multigene FMO family could be, at least in part, also the basis of the diverse properties of auxin. Although *yucca6-1D* plants display epinastic cotyledons, elongated hypocotyls, and strong apical dominance that are all phenotypes

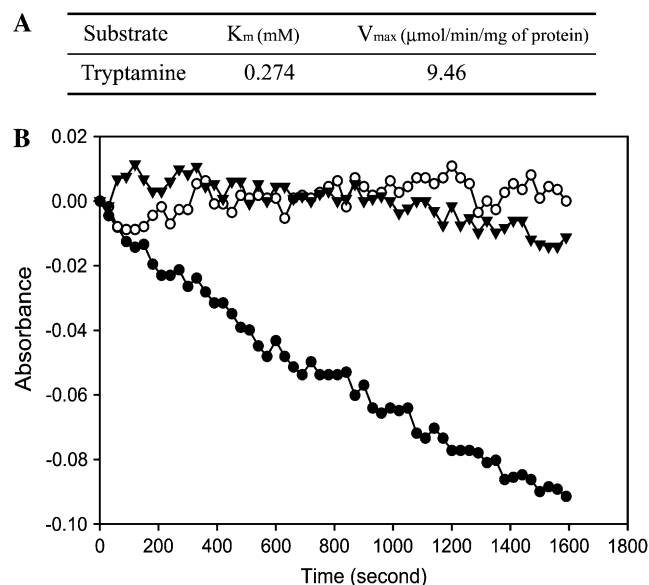


Figure 7. Characteristics of typtamine-dependent oxidation of NADPH catalyzed by MBP:YUCCA6 expressed in *E. coli*. A, Kinetic parameters (K_m and V_{max}) for typtamine-dependent oxidation of NADPH catalyzed by YUCCA6-maltose-binding fusion proteins. The kinetic parameters were calculated from initial velocity measurements by following substrate-dependent consumption of NADPH at pH 8.0 with 0.1 mM, 1.0 mM, 2 mM, 2.5 mM, 5 mM, and 10 mM concentrations of tryptamine described in "Materials and Methods." Reactions were carried out for 4 min, and initial velocities were estimated from slopes of consumption curves. B, Velocity of NADPH consumption catalyzed by MBP (control) and YUCCA6-maltose-binding fusion proteins using 2 mM tryptamine and MBP:YUCCA6 using 1 mM IAN. MBP (white circle) and MBP:YUCCA6 (black circle) proteins were incubated in reaction mixtures containing 0.1 mM NADPH and 2 mM tryptamine in 50 mM potassium phosphate buffer, pH 8.0, at 22°C for 30 min. Velocity of MBP:YUCCA6 proteins at 1 mM IAN (black triangle) was measured in the same conditions using IAN instead of tryptamine.

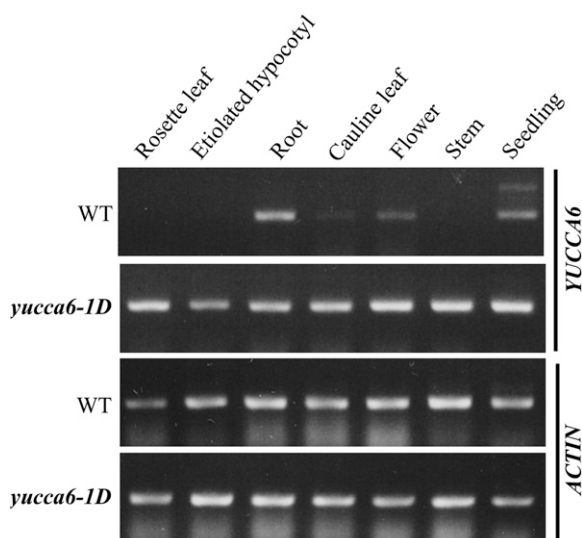


Figure 8. RT-PCR analysis for expressions of *YUCCA6* transcripts in different organs of wild type and *yucca6-1D*. Seven-day-old seedlings of wild type and *yucca6-1D* grown on MS media with or without light were sampled for RNA extraction for seedlings and etiolated hypocotyls, and designated tissues from 8-week-old soil-grown mature plants were harvested for RNA extraction. *ACTIN* was used as a control for loading.

similar to those of other *yucca* activation mutants (*yucca1-5*), *yucca6* plants do not have short and hairy roots and are not hookless when grown in the dark, which are phenotypes that have been observed in *yucca1*. Compared to the wild type, the *yucca6* plants also display some very unique mutant phenotypes such as twisted cauline leaves and larger seeds and much more extreme apical dominance.

We were very careful to interpret phenotypes of *yucca6-1D* because they are transgenic plants that overexpress *YUCCA6* by a 35S activation vector. However, most of the typical auxin overproduction phenotypes, as well as unique phenotypes that we observed in *yucca6-1D*, were consistent with the phenotypes observed in a second mutant allele, *yucca6-2D*, and in 35S::*YUCCA6* transgenic plants.

Specific phenotypes observed with different *yucca* mutants may result from different endogenous auxin levels in specific organs, tissues, or even cells. This could be caused by the relative activation of the promoters of *YUCCA* gene family members in different mutants. It is possible that even small differences in *YUCCA* gene expression in specific tissues or cells could dramatically affect phenotypes.

IAA is known to be synthesized in both roots and shoots of *Arabidopsis* (Müller et al., 1998; Ljung et al., 2005), but whether different biosynthesis pathways are used in different tissues is still unknown. *YUCCA6* transcript is very abundant in wild-type roots, and the free IAA level is not increased in roots by overexpression of *YUCCA6* (Figs. 5 and 8). Other tissues, especially inflorescences, show dramatically increased *YUCCA6* transcript and IAA levels in the *yucca6*

activation mutant. As *YUCCA* family members exhibit different expression patterns (Cheng et al., 2006), plants may utilize several gene members to efficiently synthesize auxin where it is necessary.

The unique features of *yucca6-1D* also could be associated with altered auxin polar transport. The *iaaM/iaaH* transgenic lines containing 2-fold elevated auxin levels exhibit phenotypes such as elongated hypocotyls but have normal root growth. Reduced basipetal polar auxin transport appeared to be required for normal root growth in *iaaM/iaaH* transgenic plants (van der Graaff et al., 2003). Experiments with radiolabeled IAA detected no differences in polar auxin transport in *yucca6* mutants compared to wild-type seedlings (data not shown). Because polar transport of auxin is clearly critical to normal growth and development (Christensen et al., 2000; Friml and Palme, 2002; Friml et al., 2002, 2004), it is possible that auxin polar transport in other *yucca* mutants could be changed and may affect phenotypes. However, no evidence for this has been reported.

The normal growth of *yucca6-1D* shoots under dark conditions and in roots could result from regulation of *YUCCA6* through cross talk with other hormones such as ethylene. It is known that auxin induces ethylene production, but epinastic leaves, elongated hypocotyls, and increased apical dominance were shown to be independent of putative secondary ethylene effects resulting from auxin induced ethylene production (Romano et al., 1993).

Subcellular Localization of *YUCCA6*

The subcellular localization of the enzymes involved in auxin biosynthesis may also contribute to the diverse and unique aspects of auxin action. Isotopic labeling studies have shown that Trp-dependent and -independent IAA biosynthesis does not occur in the same subcellular compartment (Rapparini et al., 2002). Trp is produced in the chloroplast, and CYP79B2, which is one of the key enzymes in Trp-dependent auxin biosynthesis, is also believed to be localized in the chloroplast. However, *Arabidopsis* *YUCCAs* are reported to be localized to the cytoplasm (Cohen et al., 2003). Our data now indicate that, indeed, *YUCCA6* is localized to the cytoplasm (Supplemental Fig. S3). Furthermore, our results suggest that *YUCCA6* may be in a subcellular compartment and not distributed throughout the cytoplasm because both *YUCCA6:GFP* and *YUCCA6:RFP* gave a punctate pattern of fluorescence that did not colocalize with any other compartments tested. The different localization of *YUCCA6* and CYP79B2 suggests that they may not be involved in the same pathway. The compartmentalization of *YUCCA6* into focused sites within the cytoplasm indicates that compartment trafficking and interaction with other subcellular sites may allow another level of control over auxin affects in growth and development.

YUCCA6 appears to be localized in an endosomal compartment, as *YUCCA6* proteins appeared to

accumulate in cytoplasmic sites that have similar appearance and abundance to sites previously identified by several endosomal markers. Endosomal compartments have been shown to function in the dynamic trafficking of auxin polar transport proteins, i.e. PIN1 and AUX1 (Kleine-Vehn et al., 2006). It is reasonable that auxin biosynthetic proteins would colocalize with auxin transport proteins in vesicular structures to concentrate (and control) delivery of auxin to plasma membrane transport sites. Such positional and functional coordination would obviously create the advantage of a much more highly concentrated (and controllable) delivery of auxin to transport sites. However, in our hands, PIN1 and AUX1 do not exhibit localizations in protoplasts consistent with what is seen in planta, so more detailed studies with stable transformed plants are required to test this hypothesis. Before further studies are completed, the localization of YUCCA6 in cytoplasmic endomembrane compartments should be interpreted with caution.

Considerable effort has been made to elucidate the auxin biosynthesis pathway with limited success. The discovery of the YUCCA family of genes and their involvement in controlling free auxin levels places the YUCCA family at the center of our knowledge of de novo auxin biosynthesis. The finding of phenotypes of *yucca6* mutant that both overlap and are unique compared with other *yucca* mutants suggests that YUCCA members, although they may overlap in their biochemical role in auxin biosynthesis, may have unique roles in plant growth and development at specific developmental stages or during specific environmental conditions. Indeed, a better understanding of auxin biosynthesis and growth regulation in plants through further analyses of the members of YUCCA family is urgently needed.

MATERIALS AND METHODS

Plant Material and Growth Condition

Arabidopsis (*Arabidopsis thaliana*) ecotype Col-0 *gI1* and Col-0 were used as the wild types of *hyt1-1D* and *hyt1-2D*, respectively. Plants were grown at 20°C to 23°C on MetroMix 360 (Scotts) under a 16-h-light/8-h-dark cycle in the greenhouse or growth chamber. For growth analyses, seedlings were grown under sterile conditions on MS media plates containing 0.8% (w/v) agar and 30 g/L Suc. For observation of root phenotypes and etiolated hypocotyls, 1.2% (w/v) agar plates were used in a vertical position. Seeds were surface sterilized with 20% (v/v) bleach for 5 min and subsequently washed five times with sterile distilled water. Seeds were cold treated for 4 d at 4°C, and then plates were placed in a growth room at 22°C on a 16-h-light/8-h-dark cycle. For genetic analysis, the genotypes of F₁ and F₂ generations were determined by epinastic cotyledon and long-narrow rosette leaf morphology. For hydroponic culture, 2.5-week-old plants were removed from soil, and roots were carefully washed with water before transfer to modified Hoagland solution (without aeration) containing 1 mM KH₂PO₄ for hydroponic culture (Liu et al., 1998). Plants were transferred to a fresh solution twice a week.

Isolation of the *sos3 hyt1-1D* Mutant

The production of a T-DNA insertion mutant (pSKI015) population of Col-0 *gI1 sos3-1* background and identification of mutations that suppress Na⁺ hypersensitivity of *sos3-1* were described (Rus et al., 2001; Miura et al., 2005).

Isolation of *hyt1-1D* and *hyt1-2D* Single Mutants

DNA flanking the left border of the inserted T-DNA in *sos3-1 hyt1-1D* plants was isolated by thermal asymmetric interlaced-PCR (Liu et al., 1995), and the entire isolated fragment was sequenced. We also designed the following primer pairs to determine a homozygous *hyt1-1D* mutant: forward, 5'-TGGTACTAATTCAGCAAT-3'; reverse, 5'-ACTCTACGTACATTGAAG-3'. To isolate a single *hyt1-1D* mutant from *sos3-1 hyt1-1D*, we crossed *sos3-1 hyt1-1D* into Col-0 *gI1* and selected a single mutant from the F₂ generation pool having *hyt1-1D* phenotypes without the *sos3* mutation through diagnostic PCR using the following primer sets: for primer set 1, which binds to the wild-type nondeleted sequence, forward 5'-ATGTGCTTTCAGTTGTACG-3' (*sos*-primer1), reverse 5'-TTTATCTTTCCTTGCATGGC-3' (*sos*-primer2); and for primer set 2, which allows recognition of the deleted sequence of *SOS3*, forward 5'-GCATGTGCTTTCAGTTACG-3' (*sos*-primer2), reverse 5'-TTTATCTTTCCTTGCATGGC-3' (*sos*-primer3). *hyt1-2D* allele in the Col-0 background was identified in the Salk Institute Genome Analysis Laboratory database, and T₃ seeds were provided by the Salk Institute Laboratory through the Arabidopsis Biological Resource Center at The Ohio State University. A homozygous line of *hyt1-2D* was selected by performing PCR using primer set LP, RP, and LBa1.

RNA Preparation and Expression Analysis

Total RNA was extracted from designated tissues using the RNeasy Plant Mini kit (Qiagen). After treatment with DNaseI (Invitrogen), 2 µg of total RNA was used for the synthesis of the first-strand cDNA using thermostable RT-PCR system and oligo(dT) as primers (Invitrogen). The gene-specific primers used to detect the transcripts were as follows: YUCCA6 forward primer 5'-ATGGATTCTGTTGGAAGAGAGAG-3', reverse primer 5'-TCAGATT-TTTTTACTTGCTCGTCT-3'; UBC (ubiquitin-conjugating enzyme; At5g25760) forward primer 5'-ATACAAAGAGGTACAGCGAG-3', reverse primer 5'-TTC-TTAGGCATAGCGCG-3'; GH3 (At5g54510) forward primer 5'-CGGAC-AAAACCGATGAGGTTG-3', reverse primer 5'-ACTCCCCATTGCTGTG-ACC-3'; GH3 (At2g23170) forward primer 5'-GCATTGAGTCGGATAAAACC-GATG-3', reverse primer 5'-TCAACGACGACGTTCTGGTGAC-3'; and IAA1 (At4g14560) forward primer 5'-ATGGAAGTCACCAATGGGCTAAC-3', reverse primer 5'-CATAAGCGAGTAGGAGCTTCGGATC-3'.

Generation of YUCCA6 Overexpression Transgenic Plants

YUCCA6 cDNAs were amplified by PCR with the following primer set: forward primer 5'-CGGGATCCATGGATTCTGTTGGAAGAGA-3' (*Bam*HI-yucca6-F); 5'-GCTGCAGTCAGATTTTTTTTACTTGATC-3' (*Pst*I-yucca6-R) reverse primer. PCR products were confirmed by nucleotide sequencing and were cloned into binary vector pCambia1300-PT between the *Pst*I and the *Bam*HI sites, and the identity of the clone insert was confirmed by sequencing. The binary vector pCambia1300-PT is a pCambia1300-based vector containing modified enzyme sites. The construct was introduced into Col-0 *gI1* wild-type plants through an *Agrobacterium tumefaciens*-mediated (strain GV3101) floral-dipping transformation method (Clough and Bent, 1998). Primary transformants were isolated on MS medium containing 30 mg/L hygromycin (Invitrogen) and transferred to soil to grow to maturity.

Histochemical GUS Analysis

Ten-day-old seedlings grown on MS media were incubated overnight in 1 mM X-gluc (5-bromo-4-chloro-3-indolyl-β-D-glucuronide; Rose Scientific) and 0.1 M potassium phosphate buffer, pH 7.5, with 0.1% (v/v) Triton X-100 (Jefferson et al., 1987). Chlorophyll was removed by washing plants several times with 70% (v/v) ethanol.

Quantification of Free IAA Levels

Free IAA determinations of seedlings were performed as described in Geisler et al. (2005). Assays of mature aerial plant tissues were performed in a similar manner but utilized 25 mg of excised tissue (from five plants) for each sample. Three sets of sampled sections were assayed for each auxin determination. Briefly, the tissue was homogenized in liquid nitrogen, diluted with 800 µL 0.05 M sodium phosphate, pH 7.0, 0.02% (w/v) sodium

diethyldithiocarbamate, combined with 4 ng ^{13}C [IAA] working standard, shaken for 15 min at 4°C, and combined with 40 μL of 1 M HCl (depending on starting weight of plant material) to a final pH of 2.7. Samples were then passed through a 0.45- μm syringe filter and applied to an Isolute C8-EC (500 mg/3 mL; no. 291-0050-B) solid-phase extraction column preconditioned by methanol/acetic acid. The sample was washed with 2 mL 10% MeOH/1% AcOH, vacuumed to remove water phase (without drying), and eluted into derivatization vials with 1 mL 70% methanol/1% acetic acid. The samples were vacuum evaporated to dryness at 30°C and methylated by adding 200 μL methanol, 1 mL dichloromethane, and 5 μL 2 M trimethylsilyl-diazomethane (in hexanes), followed by incubation at 42°C for 30 min. After neutralization with 5 μL of 2 M acetic acid/hexane to destroy excess diazomethane, samples were evaporated to dryness and resuspended in acetonitrile. Samples were analyzed by gas chromatography-mass spectrometry as described by Ljung et al. (2005), except that an Agilent/LECO gas chromatographer-mass spectrometer was used with a split injection volume of 5 μL , a transfer port temperature of 260°C, separation through a DB-5, 10-m \times 0.18-mm \times 0.20- μm column with helium carrier flow at 1 mL/min. The temperature program was 80°C for 2 min, 20°C/min to 260°C, 260°C for 2 min, and mass ranges were monitored from 70 to 200 mass-to-charge ratio. Quantitations are based on comparisons of IAA peaks to ^{13}C -IAA standards normalized to fresh weight of original sample.

RNA Extraction and Microarray Hybridization

Total RNA was isolated by a method developed for tissues with high carbohydrate content (Jaakola et al., 2001). RNAs (70 μg each) from ambient and elevated CO_2 treatments were reverse transcribed (SuperScript III; Invitrogen) and cDNAs labeled with Cy3 or Cy5 by indirect labeling (Miyazaki et al., 2004). Microarray slides with >26,000 DNA elements (70-mer gene-specific oligonucleotides; Qiagen/Operon) were used (<http://www.ag.arizona.edu/microarray/>; Miyazaki et al., 2004). To avoid bias in microarrays as a consequence of dye-related differences in labeling efficiency, dye labeling for each paired sample (mutant/control) was swapped. Two biological repeats were carried out.

Microarray Evaluation and Statistical Analysis

Signal intensities for each array element were collected (GenePix 4000B, Axon Instruments) and images analyzed (GENEPIX Pro 4.0). Spots with intensities lower than background or with an aberrant spot shape were flagged by the GENEPIX software and checked manually. The resulting GPR files were converted by EXPRESSCONVERTER V.1.5 and analyzed by the TIGR-TM4 package (<http://www.tm4.org>; Saeed et al., 2003). Total intensity normalization, Lowess (Locfit) normalization, SD regulation, and intensity filtering were done within each slide by TM4-MIDAS (version 2.18). Statistical analyses were carried out using TM4-MEV (ver. 3.0.3). In MEV, a one-class *t* test with $P = 0.01$ was carried out to reveal patterns of regulation (Hegde et al., 2000; Gong et al., 2005).

Expression and Purification of MBP:YUCCA6 Fusion Protein

The full-length YUCCA6 ORF was synthesized from Col-0 cDNA by PCR amplification and subcloned into the expression vector pMAL-c2. For PCR, two oligonucleotide primers, designated primer A (5'-CGGAATCATG-GATTTCTGTTGGAAGAGA-3') and primer B (5'-CCAAGCTTTCAGATT-TTTTTACTTGCTCGT-3'), were used. The cloning of a YUCCA6 PCR fragment into the *EcoRI* and *HindIII* sites of the vector pMAL-c2 allowed the fusion of the YUCCA6 ORF at the 5' end of sequences encoding the MBP and was named MBP:YUCCA6. Competent BL21 *Escherichia coli* cells were transformed with MBP:YUCCA6 plasmid. After inoculation with 20 mL of overnight-grown culture of BL21 containing MBP:YUCCA6, the culture was grown at 37°C until A_{600} was approximately 0.5. Then, 0.1 mM of isopropyl β -D-thiogalactopyranoside was added to the culture to induce expression of recombinant protein, and the culture was incubated for an additional 3 h at 28°C. The culture was harvested at 4°C by centrifugation at 5,000g for 10 min. The bacterial pellet was resuspended in lysis buffer (100 mM potassium phosphate, pH 8.0, 0.1 mM EDTA, 0.5 mM phenylmethylsulfonyl fluoride). The mixture was sonicated with a sonicator (550 Sonic Dismembrator; Fisher Scientific) and then centrifuged at 14,000g for 20 min to remove cellular debris. The supernatant was passed through an amylose column that was pre-

equilibrated in column buffer (100 mM potassium phosphate, pH 8.0). The amylose column was washed with column buffer. Proteins were released with elution buffer (50 mM potassium phosphate containing 10 mM maltose). MBP was used as a negative control after expression and purification by the same method as MBP:YUCCA6 protein. The protein contents were measured using Bio-Rad Protein Assay (no. 500-0006), and protein was separated by SDS-PAGE.

Analysis of Recombinant YUCCA6 Enzyme Activity

The activities of MBP:YUCCA6 and MBP proteins were measured by determining the rates of substrate-dependent NADPH oxidation consumption. Reactions were performed in 1.0 mL of reaction mixture containing 50 mM potassium phosphate, pH 8.0, 0.1 mM NADPH, 0.1 to 0.2 mg recombinant protein, and various concentrations of tryptamine in the sample cuvette and everything except tryptamine in the reference cuvette. The rates of NADPH oxidation caused by addition of tryptamine were monitored at 340 nm for 5 min at 22°C using a UV-visible spectrophotometer (model UV-1601; Shimadzu). The change in absorbance per minute was converted to micromoles NADPH consumed per minute using the extinction coefficient 6,220 $\text{M}^{-1} \text{cm}^{-1}$ for NADPH. K_m and V_{max} values were obtained by regression analysis with Sigma Plot (SPSS).

Subcellular Localization of YUCCA6

To generate *Pro_{35S}:YUCCA6:GFP* and *Pro_{35S}:YUCCA6:RFP*, the full-length YUCCA6 ORF without the stop codon was synthesized with the following primer sets: primer C (5-CTCTAGAATGGATTCTGTGGAAGAGA-3) and primer D (5-CGGATCCAGATTTTTTTTACTTGCTCGT-3) for *Pro_{35S}:YUCCA6:GFP*, and primer C and primer F (5-CGGATCCTCAGATTTTTTTTACT-TGCTC-3) for *Pro_{35S}:YUCCA6:RFP*. The PCR products were subcloned in frame at the *Bam*HI and *Xba*I sites of the 326-GFP and 326-RFP expression vectors that were kindly provided by Dr. Inhwon Hwang at POSTECH (Pohang, Korea).

Plasmids were purified using Qiagen DNA Maxi Purification kit according to the manufacturer's protocol. The plasmids were introduced into Arabidopsis protoplasts prepared from whole seedlings by polyethylene glycol-mediated transformation (Jin et al., 2001). Images were acquired using a Radiance 2100 MP Rainbow (Bio-Rad) on a TE2000 (Nikon) inverted microscope using a 60 \times 1.4 NA lens. The 488-nm line of the 4-line argon laser (National Laser) was used to excite the GFP, and the fluorescence emitted between 500 nm and 540 nm was collected. RFP fluorescence was sequentially excited using the 543-nm line of the green HeNe laser, and the emission between 560 and 610 nm was collected. Chlorophyll autofluorescence was subsequently excited with the 637-nm diode laser, and the emission greater than 660 nm was collected. A transmitted light image was also collected for reference.

Sequence data from this article can be found in the GenBank/EMBL data libraries under accession number AT5G25620 (YUCCA6).

Supplemental Data

The following materials are available in the online version of this article.

Supplemental Figure S1. RT-PCR analysis of *GH3* and *IAA1* in wild type and *yucca6-1D*.

Supplemental Figure S2. Phenotypes of loss-of-function mutation of YUCCA6 (*yucca6-3k*).

Supplemental Figure S3. Subcellular localization of YUCCA6:RFP and YUCCA6:GFP in Arabidopsis protoplasts.

ACKNOWLEDGMENTS

We thank Dr. Inhwon Hwang (POSTECH, Pohang, Korea) for providing 326GFP, F1-ATPase- γ :RFP, rat sialyltransferase:GFP, BiP:RFP, and RFP:SKL vectors, and the Salk Institute Genomic Analysis Laboratory (La Jolla, CA) for providing the sequence-indexed Arabidopsis T-DNA insertion mutants. We also thank the Dr. David Salt laboratory at Purdue (West Lafayette, IN) for assisting with the enzyme assay experiment.

Received July 3, 2007; accepted September 10, 2007; published September 20, 2007.

LITERATURE CITED

- Alonso JM, Stepanova AN, Leisse TJ, Kim CJ, Chen H, Shinn P, Stevenson DK, Zimmerman J, Barajas P, Cheuk R (2003) Genome-wide insertional mutagenesis of *Arabidopsis thaliana*. *Science* **301**: 653–657
- Bak S, Feyereisen R (2001) The involvement of two P450 enzymes, CYP83B1 and CYP83A1, in auxin homeostasis and glucosinolate biosynthesis. *Plant Physiol* **127**: 108–118
- Bak S, Nielsen HL, Halkier BA (1998) The presence of CYP79 homologs in glucosinolate-producing plants shows evolutionary conservation of the enzymes in the conversion of amino acid to aldoxime in the biosynthesis of cyanogenic glucosides and glucosinolates. *Plant Mol Biol* **38**: 725–734
- Bak S, Tax FE, Feldmann KA, Galbraith DW, Feyereisen R (2001) CYP83B1, a cytochrome P450 at the metabolic branchpoint in auxin and indole glucosinolate biosynthesis in *Arabidopsis thaliana*. *Plant Cell* **13**: 101–111
- Barlier I, Kowalczyk M, Marchant A, Ljung K, Bhalerao R, Bennett M, Sandberg G, Bellini C (2000) The *SUR2* gene of *Arabidopsis thaliana* encodes the cytochrome P450 CYP83B1, a modulator of auxin homeostasis. *Proc Natl Acad Sci USA* **97**: 14819–14824
- Bartel B, LeClere S, Magidin M, Zolman BK (2001) Inputs to the active indole-3-acetic acid pool: de novo synthesis, conjugate hydrolysis, and indole-3-butyric acid β -oxidation. *J Plant Growth Regul* **20**: 198–216
- Blakeslee JJ, Peer WA, Murphy AS (2005) Auxin transport. *Curr Opin Plant Biol* **8**: 1–7
- Boerjan W, Cervera MT, Delarue M, Beeckman T, Dewitte W, Bellini C, Caboche M, Van Onckelen H, Van Montagu M, Inzé D (1995) *superroot*, a recessive mutation in *Arabidopsis*, confers auxin overproduction. *Plant Cell* **7**: 1405–1419
- Cheng Y, Dai X, Zhao Y (2006) Auxin biosynthesis by the YUCCA flavin monooxygenases controls the formation of floral organs and vascular tissues in *Arabidopsis*. *Genes Dev* **20**: 1790–1799
- Christensen SK, Dagenais N, Chory J, Weigel D (2000) Regulation of auxin response by the protein kinase PINOID. *Cell* **100**: 469–478
- Clough SJ, Bent AF (1998) A simplified method for agrobacterium-mediated transformation of *Arabidopsis thaliana*. *Plant J* **16**: 735–743
- Cohen J, Slovin J, Hendrickson AM (2003) Two genetically discrete pathways convert tryptophan to auxin: more redundancy in auxin biosynthesis. *Trends Plant Sci* **8**: 197–199
- Davies PJ (2004) *Plant Hormones: Biosynthesis, Signal Transduction, Action*, Ed 3. Kluwer Academic Publishers, Dordrecht, The Netherlands, pp 4–6
- Delarue M, Prinsen E, Van Onckelen H, Caboche M, Bellini C (1998) *sur2* mutations of *Arabidopsis thaliana* define a new locus involved in the control of auxin homeostasis. *Plant J* **14**: 603–611
- Dharmasiri N, Dharmasiri S, Estelle M (2005) The F-box protein TIR1 is an auxin receptor. *Nature* **435**: 441–445
- Estelle M, Somerville C (1987) Auxin-resistant mutants of *Arabidopsis thaliana* with an altered morphology. *Mol Gen Genet* **206**: 200–206
- Friml J, Palme K (2002) Polar auxin transport: old questions and new concepts? *Plant Mol Biol* **49**: 273–284
- Friml J, Wisniewska J, Benkova E, Mengens K, Palme K (2002) Lateral relocation of auxin efflux regulator PIN3 mediates tropism in *Arabidopsis*. *Nature* **415**: 806–809
- Friml J, Yang X, Michniewicz M, Weijers D, Quint A, Tietz O, Benjamins R, Ouwerkerk PBF, Ljung K, Sandberg G, et al (2004) A PINOID-dependent binary switch in apical-basal PIN polar targeting directs auxin efflux. *Science* **306**: 862–865
- Geisler M, Blakeslee JJ, Bouchard R, Lee OR, Vincenzetti V, Bandyopadhyay A, Titapiwatanakun B, Peer WA, Bailly A, Richards EL, et al (2005) Cellular efflux of auxin catalyzed by the *Arabidopsis* MDR/PGP transporter AtPGP1. *Plant J* **44**: 179–194
- Gong Q, Li P, Ma S, Rupassara SI, Bohnert HJ (2005) Salinity stress adaptation competence in the extremophile *Thellungiella halophila* in comparison with its relative *Arabidopsis thaliana*. *Plant J* **44**: 826–839
- Hegde P, Qi R, Abernathy K, Gay C, Dharap S, Gaspard R, Hughes JE, Snesrud E, Lee N, Quackenbush J (2000) A concise guide to cDNA microarray analysis. *Biotechniques* **29**: 548–550
- Hellman H, Hobbie L, Chapman A, Dharmasiri S, Dharmasiri N, del Pozo C, Reinhardt D, Estelle M (2003) *Arabidopsis* AXR6 encodes CUL1 implicating SCF E3 ligases in auxin regulation of embryogenesis. *EMBO J* **22**: 3314–3325
- Jaakola L, Pirttila AM, Halonen M, Hohtola A (2001) Isolation of high quality RNA from bilberry (*Vaccinium myrtillus* L.) fruit. *Mol Biotechnol* **19**: 201–204
- Jefferson RA, Kavanagh TA, Bevan MW (1987) Histochemical localization of β -glucuronidase (GUS) reporter activity in plant tissues. *EMBO J* **6**: 3901–3907
- Jin JB, Bae H, Kim SJ, Jin YH, Goh GH, Kim DH, Lee YJ, Tse YC, Jiang L, Hwang I (2003) The *Arabidopsis* dynamin-like proteins ADL1C and ADL1E play a critical role in mitochondrial morphogenesis. *Plant Cell* **15**: 2357–2369
- Jin JB, Kim YA, Kim SJ, Lee SH, Kim DH, Cheong G, Hwang I (2001) A new dynamin-like protein, ADL6, is involved in trafficking from the trans-Golgi network to the central vacuole in *Arabidopsis*. *Plant Cell* **13**: 1511–1526
- Kepinski S, Leyser O (2005) The *Arabidopsis* F-box protein TIR1 is an auxin receptor. *Nature* **435**: 446–451
- King JJ, Stimart DP, Fisher RH, Bleecker AB (1995) A mutation altering auxin homeostasis and plant morphology in *Arabidopsis*. *Plant Cell* **7**: 2023–2037
- Kleine-Vehn J, Dhonukshe P, Swarup R, Bennett M, Friml J (2006) Subcellular trafficking of the *Arabidopsis* auxin influx carrier AUX1 uses a novel pathway distinct from PIN1. *Plant Cell* **18**: 3171–3181
- Lee KH, Kim DH, Lee SW, Kim ZH, Hwang I (2002) In vivo import experiments in protoplasts reveal the importance of the overall context, but not specific amino acid residues of the transit peptide during import into chloroplasts. *Mol Cells* **14**: 388–397
- Liu C, Muchhal US, Uthappa M, Kononowicz AK, Raghothama KG (1998) Tomato phosphate transporter genes are differentially regulated in plant tissues by phosphorus. *Plant Physiol* **116**: 91–99
- Liu YG, Mitsukawa N, Oosumi T, Whittier RF (1995) Efficient isolation and mapping of *Arabidopsis thaliana* T-DNA insert junctions by thermal asymmetric interlaced PCR. *Plant J* **8**: 457–463
- Ljung K, Hull AK, Kowalczyk M, Marchant A, Celenza J, Cohen JD, Sandberg G (2001) Biosynthesis, conjugation, catabolism and homeostasis of indole-3-acetic acid in *Arabidopsis thaliana*. *Plant Mol Biol* **49**: 249–272
- Ljung K, Hull KA, Celenza J, Yamada M, Estelle M, Normanly J, Sandberg G (2005) Sites and regulation of auxin biosynthesis in *Arabidopsis* roots. *Plant Cell* **17**: 1090–1104
- Marsch-Martinez N, Greco R, VanArkel G, Herrera-Estrella L, Pereira A (2002) Activation tagging using the En-I maize transposon system in *Arabidopsis*. *Plant Physiol* **129**: 1544–1556m
- Mikkelsen MD, Hansen CH, Wittstock U, Halkier BA (2000) Cytochrome P450 CYP79B2 from *Arabidopsis* catalyzes the conversion of tryptophan to indole-3-acetaldoxime, a precursor of indole glucosinolates and indole-3-acetic acid. *J Biol Chem* **275**: 33712–33717
- Miura K, Rus A, Sharkhuu A, Yokoi S, Karthikeyan AS, Raghothama KG, Baek DW, Koo YD, Jin JB, Bressan RA, et al (2005) The *Arabidopsis* SUMO E3 ligase SIZ1 controls phosphate deficiency responses. *Proc Natl Acad Sci USA* **102**: 7760–7765
- Miyazaki S, Fredricksen M, Hollis KC, Poroyko V, Shepley D, Galbraith DW, Long S, Bohnert HJ (2004) Transcript expression profiles of *Arabidopsis thaliana* grown under controlled conditions and open-air elevated concentrations of CO₂ and of O₃. *Field Crops Res* **90**: 47–59
- Muday GK, DeLong A (2001) Polar auxin transport: controlling where and how much. *Trends Plant Sci* **6**: 535–542
- Müller A, Hillebrand H, Weiler EW (1998) Indole-3-acetic acid is synthesized from L-tryptophan in roots of *Arabidopsis thaliana*. *Planta* **206**: 362–369
- Müller A, Weiler EW (2000) Indolic constituents and indole-3-acetic acid biosynthesis in the wild-type and a tryptophan auxotroph mutant of *Arabidopsis thaliana*. *Planta* **211**: 855–863
- Normanly J, Cohen JD, Fink GR (1993) *Arabidopsis thaliana* auxotrophs reveal a tryptophan-independent biosynthetic pathway for indole-3-acetic acid. *Proc Natl Acad Sci USA* **90**: 10355–10359
- Park WJ, Kriechbaumer V, Müller A, Piotroski M, Meeley RB, Gierl A, Glawichnig E (2003) The nitrilase ZmNIT2 converts indole-3-acetonitrile to indole-3-acetic acid. *Plant Physiol* **133**: 794–802
- Rapparini F, Tam YY, Cohen J, Slovin JP (2002) IAA metabolism in *Lemna gibba* undergoes dynamic changes in response to growth temperature. *Plant Physiol* **128**: 1410–1416
- Romano CP, Cooper ML, Klee HJ (1993) Uncoupling auxin and ethylene effects in transgenic tobacco and *Arabidopsis* plants. *Plant Cell* **5**: 181–189
- Rus A, Yokoi S, Sharkhuu A, Reddy M, Lee BH, Matsumoto TK, Koiwa H, Zhu JK, Bressan RA, Hasegawa PM (2001) AtHKT1 is a salt tolerance determinant that controls Na⁺ entry into plant roots. *Proc Natl Acad Sci USA* **98**: 14150–14155

- Saeed AL, Sharov V, White J (2003) TM4: a free, opensource system for microarray data management and analysis. *Biotechniques* **34**: 374–378
- Schmid M, Davison TS, Henz SR, Pape UJ, Demar M, Vingron M, Schölkopf B, Weigel D, Lohmann JU (2005) A gene expression map of *Arabidopsis thaliana* development. *Nat Genet* **37**: 501–506
- Smolen G, Bender J (2002) *Arabidopsis* cytochrome P450 *cyp83B1* mutations activate the tryptophan biosynthetic pathway. *Genetics* **160**: 323–332
- Swarup R, Bennett M (2003) Auxin transport: the fountain of life in plants? *Dev Cell* **5**: 824–826
- Tobeña-Santamaria R, Blied M, Ljung K, Sandberg G, Mol JNM, Souer E, Koes R (2002) FLOOZY of petunia is a flavin mono-oxygenase-like protein required for the specification of leaf and flower architecture. *Genes Dev* **16**: 753–763
- Ulmasov T, Murfett J, Hagen G, Guilfoyle TJ (1997) Aux/IAA proteins repress expression of reporter genes containing natural and highly active synthetic auxin response elements. *Plant Cell* **9**: 1963–1971
- van der Graaff E, Boot K, Granbom R, Sandberg G, Hooykaas PJJ (2003) Increased endogenous auxin production in *Arabidopsis thaliana* causes both earlier described and novel auxin-related phenotypes. *J Plant Growth Regul* **22**: 240–252
- Woodward A, Bartel B (2005) Auxin: regulation, action, and interaction. *Ann Bot (Lond)* **95**: 707–735
- Woodward C, Bemis SM, Hill EJ, Sawa S, Koshiba T, Torii K (2005) Interaction of auxin and ERECTA in elaborating Arabidopsis inflorescence architecture revealed by the activation tagging of a new member of the YUCCA family putative flavin monooxygenases. *Plant Physiol* **139**: 192–203
- Yamamoto Y, Kamiya N, Morinaka Y, Matsuoka M, Sazuka T (2007) Auxin biosynthesis by the YUCCA genes in rice. *Plant Physiol* **143**: 1362–1371
- Yang X, Lee S, So JH, Dharmasiri S, Dharmasiri N, Ge L, Gensen C, Hangarter R, Hobbie L, Estelle M (2004) The IAA1 protein is encoded by AXR5 and is a substrate of SCF (TIR1). *Plant J* **40**: 772–782
- Zhao Y, Christensen SK, Fankhauser C, Cashman JR, Cohen JD, Weigel D, Chory J (2001) A role for flavin monooxygenase-like enzymes in auxin biosynthesis. *Science* **291**: 306–309
- Zhao Y, Hull AK, Gupta NR, Goss KA, Alonso J, Ecker JR, Normanly J, Chory J, Celenza IL (2002) Trp-dependent auxin biosynthesis in Arabidopsis: involvement of cytochrome P450s CYP79B2 and CYP79B3. *Genes Dev* **16**: 3100–3112